ANALYTICAL BIOCHEMISTRY 203, 295–301 (1992)

Boundary Analysis in Sedimentation Transport Experiments: A Procedure for Obtaining Sedimentation Coefficient Distributions Using the Time Derivative of the Concentration Profile

Walter F. Stafford III

Department of Muscle Research, Boston Biomedical Research Institute, 20 Staniford Street, Boston, Massachusetts 02114; and Department of Neurology, Harvard Medical School, Boston, Massachusetts 02115

Received December 6, 1991

A procedure is described for computing sedimentation coefficient distributions from the time derivative of the sedimentation velocity concentration profile. Use of the time derivative, $(\partial c/\partial t)_r$, instead of the radial derivative, $(\partial c/\partial r)_t$, is desirable because it is independent of time-invariant contributions to the optical baseline. Slowly varying baseline changes also are significantly reduced. An apparent sedimentation coefficient distribution (i.e., uncorrected for the effects of diffusion), $g^*(s)$, can be calculated from $(\partial c/\partial t)_r$ as

$$g^*(s)_t = \left(\frac{\partial c}{\partial t}\right)_{corr}\left(\frac{1}{c_0}\right)\left(\frac{\omega^2 t^2}{\ln(r_m/r)}\right)\left(\frac{r}{r_m}\right)^2,$$

where s is the sedimentation coefficient, ω is the angular velocity of the rotor, c_0 is the initial concentration, r is the radius, r_m is the radius of the meniscus, and t is time. An iterative procedure is presented for computing $g^*(s)_t$ by taking into account the contribution to $(\partial c/\partial t)_r$ from the plateau region to give $(\partial c/\partial t)_{corr}$. Values of $g^*(s)_t$ obtained this way are identical to those of $g^*(s)$ calculated from the radial derivative to within the roundoff error of the computations. Use of $(\partial c/\partial t)_r$, instead of $(\partial c/\partial r)_t$, results in a significant increase (>10-fold) in the signal-to-noise ratio of data obtained from both the uv photoelectric scanner and Rayleigh optical systems of the analytical ultracentrifuge. The use of $(\partial c/\partial t)_r$ to compute apparent sedimentation coefficient distributions for purposes of boundary analysis is exemplified with an antigen–antibody system. © 1992 Academic Press, Inc.

Analysis of particle size distributions has been an important use of the analytical ultracentrifuge since its inception in the early 1920s by Svedberg and Nichols (1) and Svedberg and Rinde (2,3). In 1942, Bridgman (4) first presented an equation for computing sedimentation coefficient distributions from refractive index gradient curves. The Bridgman equation was exploited extensively in the 1950s especially by Baldwin and Williams (5). The following report describes the use of the time derivative of the concentration distribution to compute sedimentation coefficient distributions either from optical density profiles as a function of radius obtained from the uv photoelectric scanning system or from fringe deflections as a function of radius from the Rayleigh interferometric optical system. The development of on-line Rayleigh interferometric optical systems (6–8) has made it possible to acquire and analyze data rapidly. Analytical procedures that previously required a large amount of time and effort now can be carried out routinely; the on-line computation of sedimentation coefficient distributions has become possible. The relationship for $g^*(s)_t$ presented below was first presented at the Workshop on Ultracentrifugation held at the 1989 Biophysical Society meeting in Cincinnati (9) and also at the 1990 International Biophysics Congress in Vancouver (1990) (10). The equation presented in the latter abstract contained a typographical error.

The following quantity is defined as the normalized differential sedimentation coefficient distribution

$$\frac{dc(s)/c_0}{ds}\left(\frac{r}{r_m}\right)^2 \equiv g(s)_j,$$

where c is the concentration on the c-scale, c_0 is the initial loading concentration, s is the sedimentation coefficient, r is the radius, r_m is the radius of the meniscus,

0003-2697/92 $5.00

and $j = r$ or t depending on whether it is calculated from $\partial c/\partial r$ or $\partial c/\partial t$, respectively. The function $g(s)$ gives the weight fraction of material, $g(s)ds$, sedimenting with sedimentation coefficients between s and $s + ds$. The integral distribution curve is given by

$$G(s) \equiv \int_{z=0}^{z=s} g(z)dz.$$

In those cases for which diffusion contributes significantly to boundary spreading, the distribution functions are referred to as apparent distributions and denoted with an asterisk as $g^*(s)$ or $G^*(s)$, respectively. We consider both types of system, with and without diffusion, below. Extrapolation methods for dealing with the effects of diffusion on the $g^*(s)$ patterns will be treated elsewhere.

The concentration distribution of the sedimenting material can be viewed either as a function of radius at fixed, particular instants of time or as a function of time at fixed, specified values of radius. As shown below, apparent sedimentation coefficient distributions can be obtained from either the radial or the temporal variation of the concentration distributions. The main advantage of using the time dependence is that the precision of both the uv photoelectric scanner and the Rayleigh optical system is increased by a factor of from 10 to 100. This increase in precision can be achieved because the differentiation process results in complete elimination of the time-independent optical baseline components. Analysis of the time dependence of the concentration profiles to solve the Lamm equation has been exploited by Bethune and co-workers (11–13). Difference patterns have been used in the past to reduce baseline contributions of a photoelectric scanning system (14). The time dependence of the concentration at a single radial position was used by Runge *et al.* (7), using an on-line system to analyze the ATP-induced formation of an associated complex between microtubules and neurofilaments. Mächtle (15) has devised a method for determining broad particle size distributions by following light intensity at a single point using an eight-hole rotor and multiplexer system.

SIMULATION OF SEDIMENTATION PATTERNS

Simulated sedimentation patterns were computed by the finite element method of Claverie *et al.* (16) (programs kindly supplied by Dr. David Cox) for various ideal noninteracting systems. The patterns shown below were computed with a grid spacing of 400 points/cm and with a sedimentation time interval of 1 s between iterations.

For the case of a Gaussian distribution of s, with $D = 0$ for each component, the profiles were computed from the conditions that the boundary position for each component be given by Eq. [7] and that the plateau concentration, $c_{p,i}$, for each component obey the relation

$$c_{p,i} = c_{0,i}\exp(-2\omega^2 s_i t).$$

The boundary was constructed from 1000 components at intervals of 0.1 S with the values of $c_{0,i}$ given by the Gaussian distribution function. These were summed over all species to give the simulated concentration profile. Values of $\partial c/\partial t$ were approximated by subtracting pairs of these profiles spaced closely in time. The values of $\partial c/\partial t$ were converted to $\hat{g}(s)$ using Eq. [17]. These values of $\hat{g}(s)$ were used to correct the values of $(\partial c/\partial t)_r$ for the "plateau" contribution as described below using Eqs. [18] and [19].

DERIVATION OF THE RELATION FOR $g^*(s)$ OBTAINED FROM $\partial c/\partial t$

The following derivation is similar to that given by Fujita (17) for the Bridgman equation (see Eq. [21], below). First, we define the variable, s^*, as the radial coordinate through the following relationship for the case of a single, hydrodynamically ideal component with zero diffusion coefficient. The distinction between the sedimentation coefficient of an individual component, s, and this coordinate, s^*, must be kept in mind. In the case of zero diffusion coefficient, $s^* = s$ at the boundary position and we have

$$s^* = \frac{1}{\omega^2 t^*}\ln(r^*/r_m). \qquad [1]$$

We can define the implicit function

$$F(r^*, s^*, t^*) = \ln(r^*/r_m) - \omega^2 s^* t^* = 0 \qquad [2]$$

so that at any given time, t^*, r^* corresponds to the position of the boundary or conversely, and at any given radius, r^*, t^* corresponds to the time at which the boundary is located at r^*. Since

$$dF = \left(\frac{\partial F}{\partial r^*}\right)dr^* + \left(\frac{\partial F}{\partial s^*}\right)ds^* + \left(\frac{\partial F}{\partial t^*}\right)dt^*, \qquad [3]$$

we have

$$\frac{dt^*}{ds^*} = -\frac{(\partial F/\partial s^*)_{r^*}}{(\partial F/\partial t^*)_{r^*}} = -\frac{t^*}{s^*} = \frac{\omega^2 t^{*2}}{\ln(r_m/r^*)}. \qquad [4]$$

Now, assuming an infinitely long centrifuge cell, the time dependence of the concentration at an arbitrarily fixed position, r, in the cell, for the case of $D = 0$, for a single component is given by

$$c_r(t) = c_0 \exp(-2\omega^2 st)\, U(t^* - t), \qquad [5]$$

where $c_r(t)$ is the concentration at radial position r as a function of time, c_0 is the initial concentration, ω is the angular velocity of the rotor, s is the sedimentation coefficient, and t is time. $U(t^* - t)$ is the Heaviside unit step function defined by

$$U(t^* - t) = 1, \quad 0 < t < t^*,$$
$$U(t^* - t) = 0, \quad t^* < t, \qquad [6]$$

where t^* is the time at which the boundary passes the point r. We can also write that the position of the boundary is given by

$$r^* = r_m \exp(\omega^2 s t^*) \qquad [7]$$

so that at t^*, $r = r^*$. Note that s is not starred in Eqs. [5] and [7] since it is the actual value of s for the component under consideration.

Differentiating Eq. [5] with respect to time at constant r, we have

$$-\frac{\partial c}{\partial t} = c_0 \exp(-2\omega^2 st)\,\delta(t^* - t) + 2\omega^2 s c_0 \exp(-2\omega^2 st)\, U(t^* - t), \qquad [8]$$

where $\delta(t^* - t)$ is the Dirac delta function defined as

$$\delta(t^* - t) = \infty, \quad \text{for } t = t^*,$$
$$\delta(t^* - t) = 0, \quad \text{for } t \neq t^*. \qquad [9]$$

The delta function also has the properties that

$$\int_{t=-\infty}^{t=+\infty} \delta(t^* - t)\, dt = 1, \qquad [10]$$

$$\int_{t=-\infty}^{t=+\infty} f(t)\,\delta(t^* - t)\, dt = f(t^*), \qquad [11]$$

and [cf. Arfken (18) or Born and Wolf (19)]

$$\delta(t - t^*) = \left|\frac{dt(s)}{ds}\right|^{-1} \delta(s - s^*), \qquad [12]$$

where $dt(s)/ds$ is given by Eq. [4].

For the case of a continuous distribution of s, we arrive at the derivative of the total macromolecular concentration at each point by integrating over all values of s using Eqs. [4] and [12]:

$$-\frac{\partial c}{\partial t} = \int_{s^*=0}^{s^*=\infty} g(s^*) c_0 \exp(-2\omega^2 s^* t)\left(\frac{\ln(r^*/r_m)}{\omega^2 t^{*2}}\right) \times \delta(s - s^*)\, ds^* + 2\omega^2 \int_{s^*=0}^{s^*=\infty} s^* g(s^*) c_0 \times \exp(-2\omega^2 s^* t)\, U(s^* - s)\, ds^*, \qquad [13]$$

where $U(s^* - s) = 1$ for $s < s^*$ and $U(s^* - s) = 0$ for $s > s^*$; c_0 is the total loading concentration and the concentration of each component is given by $g(s)c_0$ (see Eq. [11]).

Carrying out the integration, relying on Eqs. [7] and [11], and specifying limits of integration for the second term, we have

$$-\frac{\partial c}{\partial t} = g(s^*) c_0 \exp(-2\omega^2 s^* t)\left(\frac{\ln(r^*/r_m)}{\omega^2 t^2}\right) + 2\omega^2 \int_{s=0}^{s=s^*} g(s) s c_0 \exp(-2\omega^2 st)\, ds. \qquad [14]$$

Rearranging, we have

$$g(s^*) = \frac{\partial c/\partial t + 2\omega^2 \int_{s=0}^{s=s^*} g(s) s c_0 \exp(-2\omega^2 st)\, ds}{c_0 \exp(-2\omega^2 s^* t)((\ln(r_m/r^*))/\omega^2 t^{*2})}. \qquad [15]$$

The first term in the numerator represents the observed, total time derivative of the concentration profile, which includes the contribution from the plateau region at s^*. The second term represents the contribution from the plateau region only. Therefore, the numerator is equal to the sum of the contribution from each of the components at its boundary position only. This function can be computed easily by iteration: .

First, we define the unnormalized distribution function as

$$\hat{g}(s^*) = g(s^*)_t c_0 \exp(-2\omega^2 s^* t). \qquad [16]$$

On the first iteration, the integral in the numerator is set to zero, so that

$$\hat{g}(s^*) \cong \frac{\partial c}{\partial t}\left(\frac{\omega^2 t^{*2}}{\ln(r_m/r^*)}\right). \qquad [17]$$

This approximate value of $\hat{g}(s^*)$ is then used in the integral on the second iteration to compute a closer approximation as

$$\hat{g}(s^*(r)) = \frac{\partial c(r^*)/\partial t + 2\omega^2 \int_{r_m}^{r^*} s^*(r)\hat{g}(s^*(r))\, ds^*(r)}{((\ln(r_m/r^*)/\omega^2 t^{*2})}. \qquad [18]$$

The new value of $\hat{g}(s^*)$ is then used to recompute the integral and the procedure is repeated until convergence

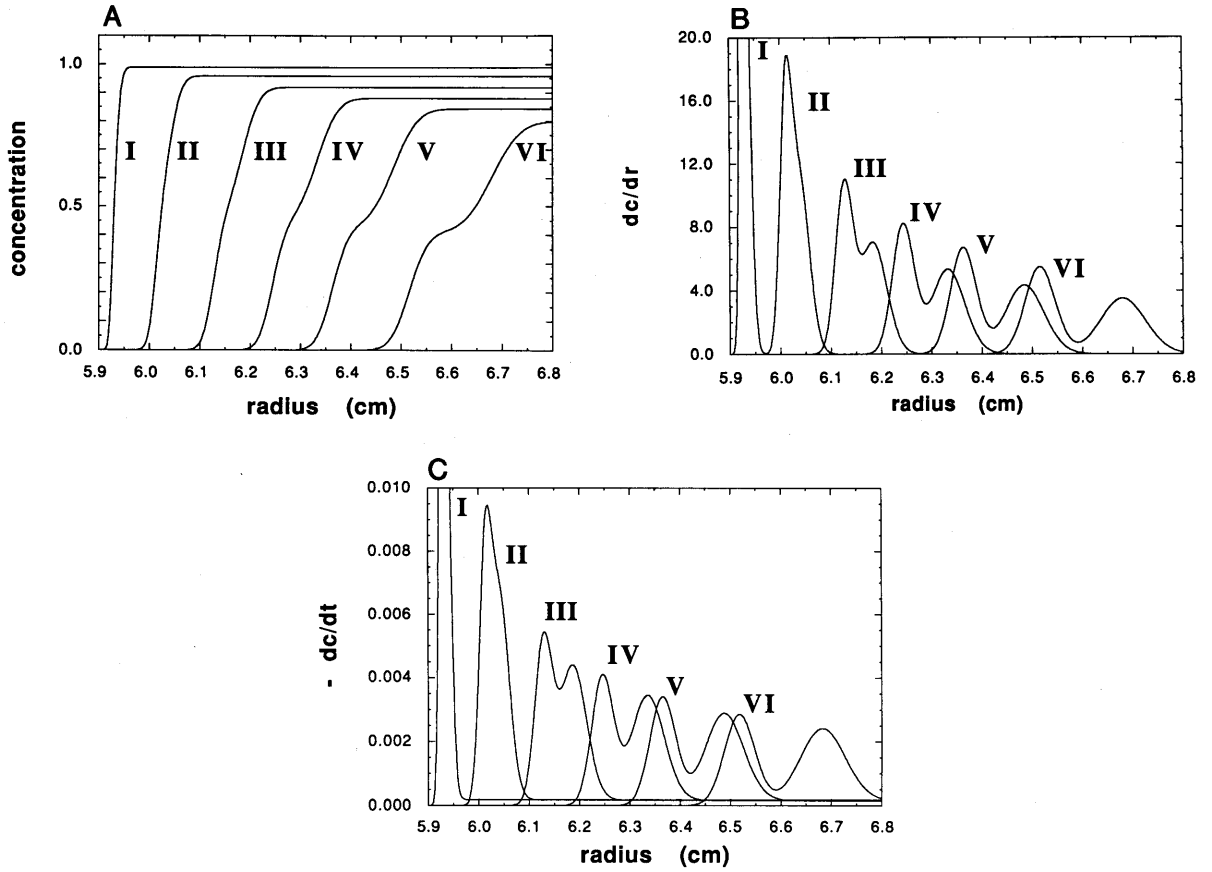

FIG. 1. Simulated sedimentation patterns for a system composed of two species: $s_1 = 20.0$ S with $D_1 = 2.0$ F ($M_1 = 900$ kDa) and $s_2 = 25.0$ S with $D_2 = 5.0$ F ($M_2 = 450$ kDa). Speed = 60,000 rpm. Roman numerals I–VI are for times of sedimentation of 60, 240, 480, 720, 960, and 1260 s, respectively. (A) Concentration vs radius profiles for various times of sedimentation. (B) Plots of the radial derivative vs radius for the same system at the corresponding times of sedimentation. (C) Plots of the time derivative vs radius at the corresponding times of sedimentation. One feature to note is that the value of $\partial c/\partial t < 0$ in the region centrifugal to the boundary and decreases in magnitude with time. The value of $\partial c/\partial t$ in this region is proportional to the product of the weight average sedimentation coefficient and the concentration in that region. The value $\partial c/\partial t$ must be corrected for this contribution. The procedure is presented in the text.

is reached. The final, corrected value of $\hat{g}(s^*)$ is then converted to $g(s^*)_t$ (after dropping the stars, but keeping them in mind), using

$$g(s)_t = \frac{\hat{g}(s)}{c_0 \exp(-2\omega^2 s t)}. \qquad [19]$$

In practice, three iterations will give satisfactory convergence.

Equation [15] is analogous to the Bridgman equation below (Eq. [21]) if one notes that the iteration procedure effectively corrects the time derivative for the contribution from the plateau region so that

$$g(s)_t = \left(\frac{\partial c}{\partial t}\right)_{\text{corr}} \left(\frac{1}{c_0}\right) \left(\frac{\omega^2 t^2}{\ln(r_m/r)}\right) \left(\frac{r}{r_m}\right)^2. \qquad [20]$$

Often, at very low concentrations, c_0 is not known accurately and is left out of the computation. The area under the $g(s)$ curve, in this case, will give the initial concentration. The distribution can be normalized using this value of the initial concentration.

The equation of Bridgman (4,17), used for computing $g(s)$ from the radial derivative, is

$$g(s)_r = \left(\frac{\partial c}{\partial r}\right) \left(\frac{1}{c_0}\right) (\omega^2 r t) \left(\frac{r}{r_m}\right)^2. \qquad [21]$$

In cases for which diffusion cannot be ignored, these functions will be apparent sedimentation coefficient distributions, as mentioned above, and designated as such with an asterisk as either $g^*(s)_t$ or $g^*(s)_r$. The apparent distribution function, without further correction for diffusion, is useful for boundary analysis.

RESULTS

We first examine two cases of simulated sedimentation and then an experimental example.

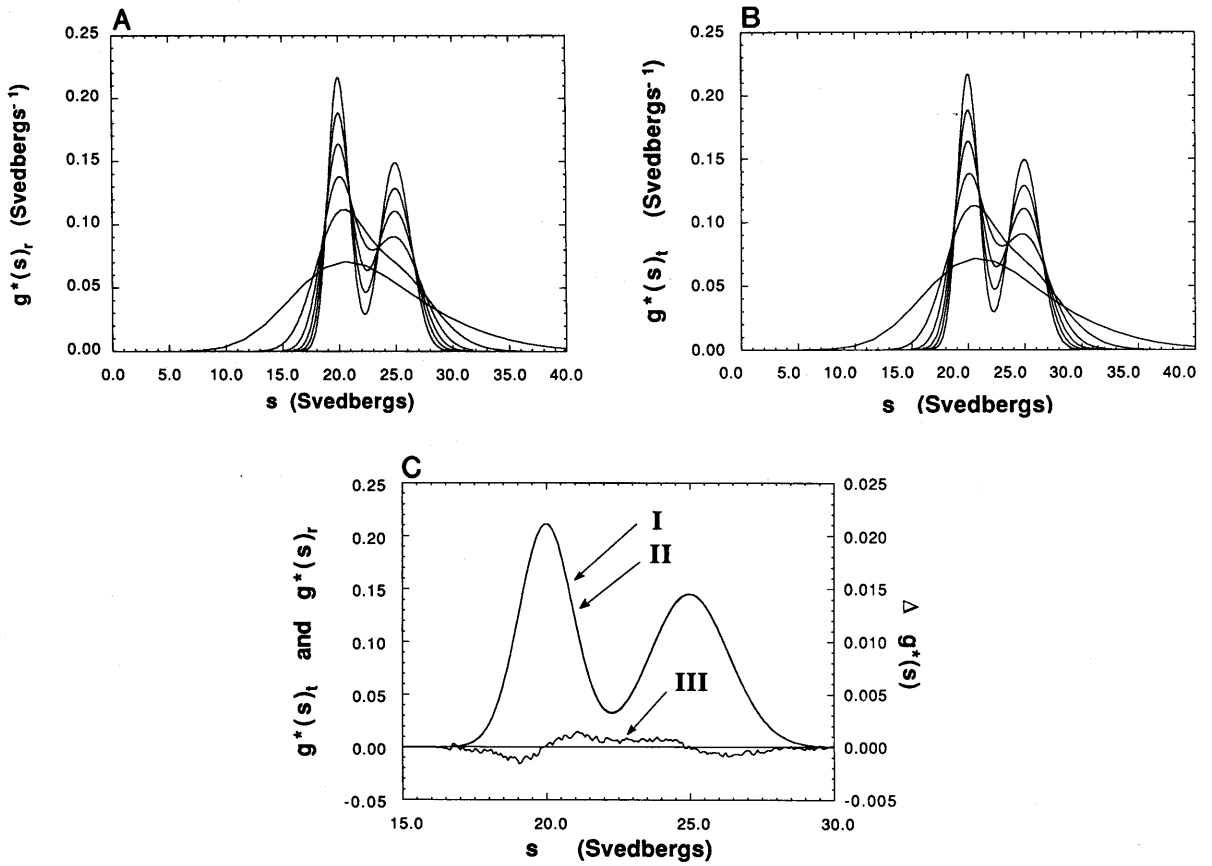

FIG. 2. The apparent sedimentation coefficient distributions, $g^*(s)$, computed from the patterns shown in Fig. 1. (A) Plots of $g^*(s)_r$ computed from $\partial c/\partial r$ using the Bridgman equation (Eq. [21]). (B) Plots of $g^*(s)_t$ computed using Eq. [15] and the iterative procedure represented by Eq. [18]. (C) Comparison of $g^*(s)_r$ and $g^*(s)_t$ showing that the two methods give equivalent distribution functions. Left y-axis: (I) $g^*(s)_r$ and (II) $g^*(s)_t$. Right y-axis: (III) $\Delta g^*(s) = g^*(s)_r - g^*(s)_t$.

Simulated Sedimentation Patterns

Two systems were simulated: the first is for a system composed of two components, one having $s_1 = 20$ S, $D_1 = 2.0$ F and the other $s_2 = 25$ S and $D_2 = 5.0$ F, present in equal amounts; the second simulated case is for a system having a nearly continuous Gaussian distribution of s (1000 components with $\mu = 50$ S and $\sigma = \pm 10$ S) and no diffusion.

The first system was simulated for the purpose of comparing $g^*(s)_t$ with $g^*(s)_r$, in order to test the iteration procedure to determine whether it gives the same results as the Bridgman equation when D is not negligible. When the iteration procedure is applied three times, the corrected values of $g^*(s)_t$ are nearly identical to those calculated from $g^*(s)_r$ using the Bridgman equation (4). Figure 1 shows a series of sedimentation patterns for the two species system. Figure 1A shows the concentration as a function of radius at various times and Figs. 1B and 1C show plots of $(\partial c/\partial r)_t$ and $(\partial c/\partial t)_r$, respectively, as a function of time for the corresponding curves in Fig. 1A.

Figure 2 shows $g(s)$ curves computed from $(\partial c/\partial r)_t$ using the Bridgman equation and from $(\partial c/\partial t)_r$ using equation [15] after three iterations for the system shown in Fig. 1. Figure 2C shows a comparison plot. The curves obtained by the two methods are nearly identical to within the roundoff error of the simulations.

The second system, one having a nearly continuous Gaussian distribution of s ($\mu = 50$ S, $\sigma = 10$ S) and no diffusion, is shown in Fig. 3. The original, true $g(s)$ curve is shown along with the uncorrected and corrected $g(s)$ curves computed as described above. The agreement between the corrected and the original $g(s)$ used to generate the concentration profiles is very good. These two examples show that this method using $\partial c/\partial t$ to compute $g^*(s)_t$ gives reliable results in cases of both negligible and nonnegligible diffusion.

Experimental Example

The method for computing $g^*(s)$ from $\partial c/\partial t$ was demonstrated experimentally by examining the interaction

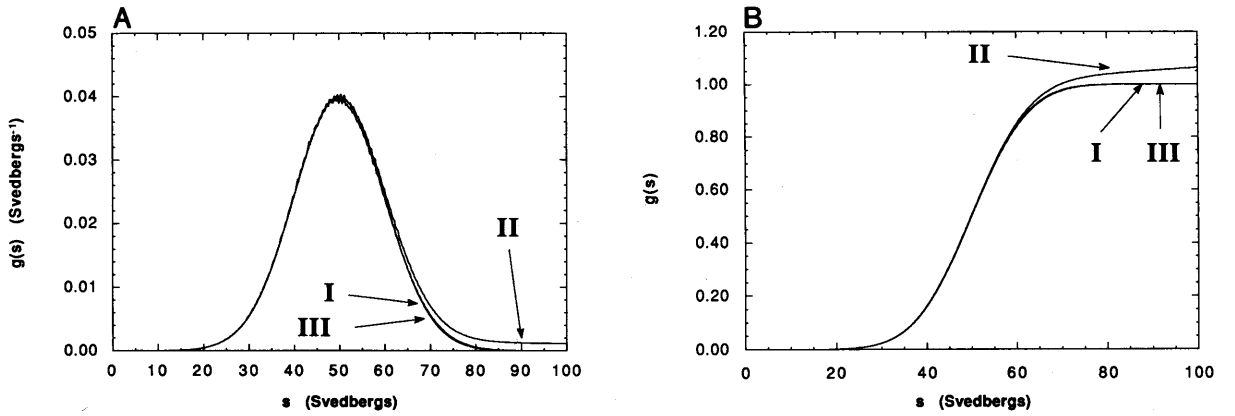

FIG. 3. Comparison of $g(s)_t$ to the true distribution, $g(s)$. Sedimentation coefficient distribution function for a simulated system composed of Gaussian distribution of 1000 species having a mean sedimentation coefficient of 50 S and a standard deviation of ±10 S. (A) Differential distribution. (B) Integral distribution obtained by integrating the curves in (A). The sedimentation patterns where generated as described in the text. (I) The true distribution of sedimentation coefficients used to generate simulated sedimentation profiles. (II) The distribution function uncorrected for the contribution to the "plateau" region centrifugal to each boundary as described in the text. (III) The corrected distribution function. (The "jagged" character of the curve at the maximum of the peak arises because the distribution is computed from the difference of two concentration profiles, each of which comprises a series of discrete step functions. The step size is maximal at the peak of the distribution function. This is an artifact of the simulation procedure and could be reduced by using more species in the original distribution.)

between diphtheria toxin and anti-diphtheria toxin immunoglobin G. Figure 4 shows the $g^*(s)_t$ patterns obtained using an on-line Rayleigh optical system (8) with three cells in a four-hole rotor. Rayleigh interferograms of all three cells were acquired and analyzed every 60 s. Values of $\Delta c/\Delta t$ were computed by subtracting pairs of concentration profiles closely spaced in time. These values of $\Delta c/\Delta t$ were substituted into Eq. [15] for $\partial c/\partial t$ to obtain $\hat{g}(s)_t$, which was then corrected using Eqs. [18] and [19] for the plateau contribution with three iterations to give $g^*(s)_t$. Each of the curves shown in Fig. 4 was obtained from the average of several data sets obtained over a small time interval (20). The details of the averaging procedure will be presented elsewhere.

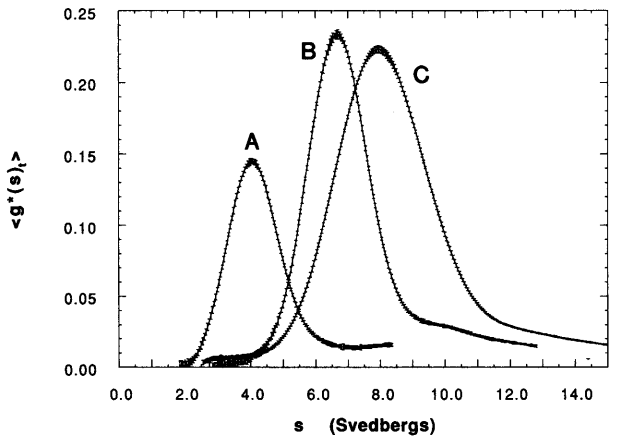

FIG. 4. Demonstration of the technique: Sedimentation velocity analysis of complex formation between anti-diphtheria toxin immunoglobin G and diphtheria toxin. Sedimentation was carried out at 56,000 rpm at 20°C using an on-line Rayleigh optical system (8) and 12-mm Kel-F centerpieces with sapphire windows. (A) Diphtheria toxin alone (c_0 = 90 μg/ml; 0.32 fringes at λ = 6328 Å; t_{sed} = 5497 s), (B) anti-diphtheria toxin immunoglobin G alone (190 μg/ml; 0.66 fringes; t_{sed} = 3384 s), and (C) the mixture showing complex formation (260 μg/ml; 0.92 fringes; t_{sed} = 2793 s). The error bars are the standard error of the mean propagated from the averaging process. The data used in the computation were collected over a time interval of 600 s.

DISCUSSION

A procedure for computing apparent sedimentation coefficient distribution functions, $g^*(s)$, from the time derivative of the concentration profile has been presented. The method has the advantage over other means of boundary analysis in that it completely eliminates the time-invariant optical background contributed by the cell windows and optics of the ultracentrifuge. Because the time derivative is computed from patterns closely spaced in time, the procedure also greatly reduces slowly varying background contributions such as those from drive oil accumulation and creep of cell components affecting cell window contributions. The signal-to-noise ratio of data analyzed by this method is considerably higher than that attainable by other methods with the same optical systems. The resulting increase in precision allows boundary analysis to be carried out at lower concentrations than those otherwise attainable. This method will enable investigation of interacting and noninteracting systems in a concentration range previously inaccessible to the analytical ultracentrifuge with the uv photoelectric scanner and Rayleigh optical systems.

ACKNOWLEDGMENTS

I thank Dr. Victor Raso for kindly supplying the immunoglobin G and diphtheria toxin samples, and I thank Dr. David Yphantis for helpful critical comments. This work was supported in part by National Cancer Institute (CA 51880) and by National Institutes of Health (RR - 05711).

REFERENCES

1. Svedberg, T., and Nichols, J. B. (1923) *J. Am. Chem. Soc.* **45,** 2910–2917.
2. Svedberg, T., and Rinde, H. (1923) *J. Am. Chem. Soc.* **45,** 943–954.
3. Svedberg, T., and Rinde, H. (1924) *J. Am. Chem. Soc.* **46,** 2677–2693.
4. Bridgman, W. B. (1942) *J. Am. Chem. Soc.* **64,** 2349–2356.
5. Baldwin, R. L., and Williams, J. W. (1950) *J. Am. Chem. Soc.* **72,** 4325.
6. Laue, T. M. (1981) Ph.D. Dissertation, University of Connecticut.
7. Runge, M. S., Laue, T. M., Yphantis, D. A., Lifsics, M. R., Saito, A., Altin, M., Reinke, K., and Williams, R. C. J. (1981) *Proc. Natl. Acad. Sci. USA* **78,** 1431–1435.
8. Liu, S., and Stafford, W. F. (1992) *Biophys. J.* **61,** (#2746)A475.
9. Stafford, W. F. (1989) *Biophys. J.* **55,** Special appendix to the abstracts.
10. Stafford, W. F. (1990) Abstracts of the International Biophysics Congress, 1990, Vancouver.
11. Bethune, J. L. (1970) *Biochemistry* **9,** 2737–2744.
12. NcNeil, B. J., and Bethune, J. L. (1973) *Biochemistry* **12,** 3254–3259.
13. McNeil, B. J., and Bethune, J. (1973) *Biochemistry* **12,** 32.
14. Cohen, R., Cluzel, J., Cohen, H., Male, P., Moignier, M., and Soulie, C. (1976) *J. Biophys. Chem.* **5,** 77–96.
15. Mächtle, W. (1988) *Angew. Makromol. Chem.* **162,** 35–52.
16. Claverie, J.-M., Dreux, H., and Cohen, R. (1975) *Biopolymers* **14,** 1685.
17. Fujita, H. (1976) Foundations of Ultracentrifugal Analysis, Wiley, New York.
18. Arfken, G. (1970) *in* Mathematical Methods for Physicists, 2nd ed., p. 419, Academic Press, New York.
19. Born, M., and Wolf, E. (1980) Principles of Optics, 6th ed., Appendices IV and VI, Pergamon, New York.
20. Stafford, W. F. (1992) *Biophys. J.* **61,** (#2746)A476.